PCCP

Li^+ Transference Number and Dynamic Ion Correlations in Gylme-Li Salt Solvate Ionic Liquids Diluted with Molecular Solvents

Journal:	*Physical Chemistry Chemical Physics*
Manuscript ID	CP-ART-03-2022-001409.R1
Article Type:	Paper
Date Submitted by the Author:	27-May-2022
Complete List of Authors:	Sudoh, Taku; Yokohama National University Shigenobu, Keisuke; Yokohama National University, Chemistry Dokko, Kaoru; Yokohama National University, Department of Chemistry and Biotechnology Watanabe, Masayoshi; Yokohama National University, Chemistry andBiotechnology Ueno, Kazuhide; Yokohama National University, Department of Chemistry and Biotechnology

Phys. Chem. Chem. Phys.: Article

Li^+ Transference Number and Dynamic Ion Correlations in Glyme-Li Salt Solvate Ionic Liquids Diluted with Molecular Solvents

Taku Sudoh,[a] Keisuke Shigenobu,[a] Kaoru Dokko,[a,b] Masayoshi Watanabe,[b] and Kazuhide Ueno,[a,b,]*

[a] Department of Chemistry and Life Science, Yokohama National University,79-5 Tokiwadai, Hodogaya-ku, Yokohama 240-8501, Japan

[b] Advanced Chemical Energy Research Centre (ACERC), Institute of Advanced Sciences, Yokohama National University, 79-5 Tokiwadai, Hodogaya-ku, Yokohama 240-8501, Japan

CORRESPONDING AUTHOR FOOTNOTE: To whom correspondence should be addressed.

Telephone/Fax: +81-45-339-3951. E-mail: ueno-kazuhide-rc@ynu.ac.jp

ABSTRACT

Highly concentrated electrolytes (HCEs) have attracted significant interest as promising liquid electrolytes for next-generation Li secondary batteries, owing to various beneficial properties both in the bulk and at the electrode/electrolyte interface. One particular class of HCEs consists of binary mixtures of lithium bis(trifluoromethanesulfonyl)amide (LiTFSA) and oligoethers that behave like ionic liquids. [Li(G4)][TFSA], which comprises an equimolar mixture of LiTFSA and tetraglyme (G4), is an example. In our previous works, the addition of low-polarity molecular solvents to [Li(G4)][TFSA] was found to effectively enhance the conductivity while retaining the unique Li-ion solvation structure. However, it remains unclear how the diluents affect another key electrolyte parameter—the Li^+ transference number—despite its critical importance for achieving the fast charging/discharging of Li secondary batteries. Thus, in this study, the effects of diluents on the extremely low Li^+ transference number under anion-blocking conditions in [Li(G4)][TFSA] were elucidated, with a special focus on the polarity of the additional solvents. The concentration dependence of the dynamic ion correlations was further studied in the framework of the concentrated electrolyte theory. The results revealed that a non-coordinating diluent is not involved in the modification of the ion transport mechanism, and therefore the low Li^+ transference number is inherited by the diluted electrolytes. In contrast, a coordinating diluent effectively reduces the anti-correlated ion motions of [Li(G4)][TFSA], thereby improving the Li^+ transference number. This is the first time that the significant effects of the coordination properties of the diluting solvents on the dynamic ion correlations and Li^+ transference numbers have been reported for diluted solvate ionic liquids.

KEYWORDS: Solvate ionic liquids, battery electrolyte, glyme, transference number, anti-correlated ion motion

1. Introduction

Highly concentrated electrolytes (HCEs) with salt concentrations exceeding 3 mol dm^{-3} or that reach the saturation limit have attracted significant interest as promising liquid electrolytes for next-generation Li secondary batteries.[1-3] HCEs have been found to offer numerous advantageous properties over conventional organic electrolytes both in the bulk and at the electrode/electrolyte interface, including enhanced thermal and electrochemical stabilities,[4, 5] fast electrode kinetics,[6-9] corrosion inhibition of current collectors,[10, 11] and suppressed active material dissolution into electrolyte solutions.[12-14] Room-temperature molten solvates composed of oligoethers (glymes) and Li salts are a particular class of HCEs that exhibit ionic liquid-like thermal and physicochemical properties, and are thus referred to as solvate ionic liquids (SILs).[15] The one-to-one molar mixture of lithium bis(trifluoromethanesulfonyl)amide (LiTFSA) and tetraglyme (G4), [Li(G4)][TFSA], is the archetype of such SILs. Experimental and computational studies have elucidated the formation of the long-lived $[Li(G4)]^+$ complex cation, with the crown ether-like conformation of G4, and scarcity of the uncoordinated solvent in [Li(G4)][TFSA].[16-20] The strong Li–G4 interaction and low solvent activity are responsible for the prominent thermal and electrochemical stabilities and stable charge-discharge cycling performances of Li-ion and Li-S batteries with high Coulombic efficiency.[4, 12]

HCEs and SILs face a common challenge of low ionic transport properties because of their intrinsically high viscosity. Indeed, the conductivity of HCEs is generally more than an order of magnitude lower than that of conventional organic electrolyte solutions. In previous works, HCEs were blended with low-viscous molecular solvents to reduce the viscosity and improve the conductivity.[12, 21] It was reported that the addition of the low-polarity hydrofluoroether 1,1,2,2-tetrafluoroethyl 2,2,3,3-tetrafluoropropyl ether (HFE) to [Li(G4)][TFSA] significantly decreased the viscosity to the same level as that of organic electrolytes and increased the conductivity to ~5 mS cm^{-1}, while retaining the unique Li-ion coordination structure of the SIL. This approach is now applied to the novel electrolyte design concept of “localized

high-concentration electrolytes (LHCEs)" that achieves high conductivity without compromising the favorable electrochemical properties of the parent HCEs.[22-24]

The unique Li-ion solvation structure of SILs also has a strong impact on their ionic transport mechanism. Recent investigations on dynamic ion correlations have shown that all cross-correlated ion motions (cation-cation, anion-anion, and cation-anion) in [Li(G4)][TFSA] are anti-correlated, owing to the constraint of momentum conservation for the long-lived $[Li(G4)]^+$ cation and bulky $TFSA^-$ anion.[25, 26] This is reminiscent of the ion transport behavior of solvent-free molten salts and ionic liquids,[27, 28] and is therefore corroborating evidence for categorizing [Li(G4)][TFSA] as an SIL. In contrast, the strongly anti-correlated ion motions were found to result in a low Li^+ transference number for SILs under anion-blocking conditions. Indeed, the Li^+ transference number (or transport number by IUPAC name[29]) determined by an electrochemical method using a Li/Li symmetric cell ($t_{\mathrm{Li}}^{\mathrm{EC}}$) was extremely low (0.028) for [Li(G4)][TFSA], which is detrimental to the fast charge-discharge of Li secondary batteries.[25, 30, 31] A molecular dynamics (MD) simulation study by Bedrov et al. demonstrated that the reduction of the strongly anti-correlated motion of ions enhances the $t_{\mathrm{Li}}^{\mathrm{EC}}$ of the SILs. One of the proposed electrolyte modifications in their study was to dilute the SIL with additional solvents that do not coordinate with the Li ions.[25] It was considered that the frequent momentum exchange of the additional solvent molecules mitigates the strongly anti-correlated ion motions for the momentum conservation in the system, leading to an increase in $t_{\mathrm{Li}}^{\mathrm{EC}}$.

Despite the importance of $t_{\mathrm{Li}}^{\mathrm{EC}}$ for realizing the fast charging/discharging of Li secondary batteries,[32, 33] it remains unclear how electrolyte components, such as Li salt and solvents, influence the $t_{\mathrm{Li}}^{\mathrm{EC}}$ in organic liquid electrolytes. According to the above notion proposed by Bedrov et al.,[25] the addition of inert solvents, such as HFE to the SILs, has the potential to improve the very low $t_{\mathrm{Li}}^{\mathrm{EC}}$ and enhance the conductivity. With these facts in mind, in this study, the effects of diluting solvents on the Li^+ transference number in [Li(G4)][TFSA] were investigated. In particular, we focused on the polarity of the diluting solvents, using propylene carbonate (PC) and HFE as coordinating and non-coordinating solvents with Li

ions, respectively. The concentration dependence of the dynamic ion correlations is further studied in the framework of Roling and Bedrov's concentrated solution theory, which is defined in the laboratory frame of reference.[25, 30, 34] In this present work, the significant effects of the coordination properties of the diluting solvents on the dynamic ion correlations and Li^+ transference numbers was for the first time elucidated for the diluted SILs.

2. EXPERIMENTAL SECTION

Materials

Tetraglyme (G4; battery grade; water content, <50 ppm), propylene carbonate (PC; battery grade; water content, <50 ppm), and lithium bis(trifluoromethanesulfonyl)amide (LiTFSA; purity, >99.9%; water content, <100 ppm) were purchased from Kishida Chemical Co., Ltd. (Japan). Additionally, 1,1,2,2-tetrafluoroethyl 2,2,3,3-tetrafluoropropyl ether (HFE) was purchased from Daikin Industries Ltd. (Japan). These purified solvents and the Li salt were used as received. [Li(G4)][TFSA] was prepared by mixing stoichiometric amounts of G4 and LiTFSA and diluting the mixture with PC or HFE at the appropriate molar ratios in an inert argon-filled glovebox ([H_2O] <1 ppm; [O_2] <1 ppm).

Measurement

The self-diffusion coefficients of Li, TFSA, and the solvents were determined within error of 10% using pulse-field-gradient (PFG)-NMR, as described in our previous study.[21] A JEOL ECX-400 NMR spectrometer with a 9.4 T narrow-bore superconducting magnet and pulsed-field gradient probe was used for the measurements. The pulse field gradient magnitude (g) was calibrated using deuterated water. ^{1}H, ^{7}Li, and ^{19}F NMR spectra were recorded for the solvents, Li, and TFSA, respectively. Raman spectra were obtained using a 785 nm laser Raman spectrometer (NRS-4100, JASCO) at a resolution of ~ 4 cm^{-1} and calibrated using a polypropylene standard. The temperature of the samples was adjusted to 30 °C using a Peltier microscope stage (TS62, INSTEC) with a temperature controller (mk1000, INSTEC). The Li^+

transference number ($t_{\mathrm{Li}}^{\mathrm{EC}}$) was determined using potentiostatic polarization combined with electrochemical impedance spectroscopy.[35, 36] The experiments were performed using Li/Li symmetric cells encapsulated in R2032-type coin cells. A porous glass filter paper (Advantec, GA55, diameter = 17 mm) soaked with the electrolytes was placed between two Li foil electrodes (Honjo Metal, diameter = 16 mm). Prior to potentiostatic polarization, the impedance measurements were performed every hour, in the frequency range of 0.1 Hz–1 MHz, at an alternating voltage amplitude of 5 or 10 mV, using a ModuLab XM ECS electrochemical test system (Solartron Analytical) to monitor the stabilization of the Li electrode interface. After stabilization of the cells, a polarization curve with a potential step of 5 or 10 mV was obtained until the current reached the steady state. Subsequently, impedance spectra were recorded with a potential bias of 5 or 10 mV, to obtain the interfacial impedance of the polarized cells. The conductivity (σ_{ion}) was obtained using the complex impedance method for the frequency between 1 Hz and 500 kHz at an alternating voltage amplitude of 10 mV (VMP3, Biologic, Claix, France). The cell constants of the conductivity cells (two platinum black electrode cells) were determined using 0.01 mol dm^{-3} KCl aqueous solution at 25 °C. The salt diffusion coefficients (D_{salt}) of the electrolytes used for calculating the Onsager transport coefficients were determined using Li/Li symmetric cells. The cells were polarized at a constant current density of 0.25 mA cm^{-2} until steady state was reached, and the voltage relaxation of the cell potential was recorded after the applied current was removed. The maximum experimental error was 11%. The Li/Li$^+$ electrode potential (electromotive force, EMF) in each electrolyte was measured within error of ±2 mV with respect to the reference electrode (Li/Li$^+$ in 1 mol dm^{-3} LiTFSA/G3) using a multi-compartment concentration cell. Vycor glass was used for the junction between the reference and sample electrolytes. The value of $\mathrm{d}\varphi/\mathrm{dln}(c)$ at a given concentration was obtained from the slope of the concentration dependence of the potential, as shown in **Figure S1**. To measure the concentration dependence of the EMF, the Li salt concentration was varied while maintaining the molar ratios of G4 and the diluting solvents (PC or HFE), assuming concentration polarization in the electrochemical cells. All the above experimental cells were prepared and sealed in the glovebox and the measurements were performed at 30 °C unless otherwise noted.

3. RESULTS AND DISCUSSION

3.1 Diffusivity

In our previous study, the addition of the relatively low-polarity HFE to [Li(G4)][TFSA] was found to enhance the conductivity while retaining the $[Li(G4)]^+$ complex cation, without the glyme ligand being replaced by the diluting molecules.[21] The stability of the $[Li(G4)]^+$ complex cations was ascertained with the G4/Li-ion diffusivity ratio (D_G/D_{Li}) of unity. The concentration dependence of the self-diffusion coefficients of the components in [Li(G4)][TFSA] diluted with HFE and PC is illustrated in **Figure 1**, to highlight the Li-ion solvation structure and transport properties in the presence of the diluting solvents.

As seen in **Figure 1a**, the diffusion coefficients of Li (D_{Li}) and TFSA (D_{anion}) significantly increased with the addition of HFE, which contributed to the enhancement of σ_{ion} to a maximum value of 5.2 mS cm^{-1} at ~1.0 mol dm^{-3}.[12] The self-diffusion coefficients of G4 (D_G) were nearly identical to those of D_{Li} and D_{anion} across all the studied concentration range. The identical values of D_G and D_{Li} suggest that the $[Li(G4)]^+$ complex cations remained stable, even at the very low salt concentration (c_{Li}) of 0.06 mol dm^{-3} with 100-fold dilution with HFE. Moreover, HFE diffused much faster than the other components, indicating that it does not strongly interact with the Li ions. The dielectric constant (ε) and Gutmann's donor number (DN) for HFE were reported to be 6.7 and 1.9, respectively.[21] These solvent polarity parameters of HFE are much lower than those of G4 (ε = 7.7; DN = 17).[37] Therefore, it is reasonable to deem HFE a non-coordinating diluent for [Li(G4)][TFSA]. The inert solvent character of HFE for Li-ion solvation in [Li(G4)][TFSA]-HFE was also verified by Raman analysis, high energy X-ray scattering experiments, and MD simulations.[38] The presence of the complex cations was verified by the characteristic ring-breathing Raman band of the complex cations.[39] The strong Raman band in the range of 740–750 cm^{-1} is ascribed to the S−N symmetric stretching vibration coupled with the CF_3 bending for TFSA and is sensitive to Li^+−$TFSA^-$ interactions. It was reported that this band slightly shifts to higher frequency with the addition of HFE, suggesting a small increase in the cation-anion interactions in [Li(G4)][TFSA]-HFE.[38] Hence, the addition of HFE does not cause significant modification of the local

Li-ion solvation structure in [Li(G4)][TFSA] except for the marginal enhancement of Li^+−$TFSA^-$ interactions.

In contrast to HFE, PC has polarity parameters of ε = 65 and DN = 15,[21] of which DN is comparable to that of G4. Therefore, PC has the potential to interrupt the formation of the $[Li(G4)]^+$ complex ions in [Li(G4)][TFSA]-PC. At c_{Li} values >1.0 mol dm^{-3}, D_G remained almost equivalent to D_{Li} (**Figure 1b**). This indicates that the strong chelate effect of the multidentate G4 ligand still prevailed against the high polarity of PC to stabilize the $[Li(G4)]^+$ complex cations. However, at c_{Li} values <0.5 mol dm^{-3}, D_{Li} became the lowest value after D_G. This suggests that some of the G4 molecules dissociated from the Li ions and were replaced by PC molecules, owing to the abundance of PC at the lower c_{Li} values. The lowest value of D_{Li} also implies the formation of Li ions solvated with some PC molecules with a larger hydrodynamic radius, similar to that observed in typical organic electrolyte solutions.[40, 41] These observations were further validated with Raman spectroscopy for [Li(G4)][TFSA]-PC (**Figure S2**). The breathing mode of the $[Li(G4)]^+$ complex cations at ~867 cm^{-1} was still discernible at c_{Li} values >1.0 mol dm^{-3}, but almost disappeared at c_{Li} value of 0.34 mol dm^{-3} with 30-fold dilution with PC. The intense band derived from TFSA in the range of 740–750 cm^{-1} shifted to lower frequency, whereas the band ascribed to the symmetric ring deformation of PC at ~710 cm^{-1} shifted to higher frequency.[42] These changes in Raman bands suggest that TFSA anions coordinated to Li ions are replaced by PC at higher c_{Li}, and G4 ligands coordinated to Li ions are subsequently replaced by the additional PC with the further dilution. Thus, in contrast to [Li(G4)][TFSA]-HFE, the Li^+−$TFSA^-$ interactions became weaker in [Li(G4)][TFSA]-PC, and the dissociation degree increased with the addition of PC. Consequently, the $[Li(G4)]^+$ complex cations became unstable and the G4 ligand was replaced by PC, to some extent, in [Li(G4)][TFSA]-PC at low c_{Li}.

The increase in D_{Li} in [Li(G4)][TFSA]-PC was not significant compared to that observed in [Li(G4)][TFSA]-HFE with the addition of the diluents, owing to the higher viscosity of PC than that of HFE. In contrast, the maximum σ_{ion} value of [Li(G4)][TFSA]-PC (7.3 mS cm^{-1} at 1.0 mol dm^{-3}) was higher than that of [Li(G4)][TFSA]-HFE, owing to the high ε value of PC, which facilitated ionic

dissociation. Nevertheless, the collapse of the $[Li(G4)]^+$ complex ions in [Li(G4)][TFSA]-PC resulted in unfavorable electrochemical properties, such as lower oxidative stability and severe aluminum corrosion that deteriorates the cycling performance of Li-ion batteries.[43]

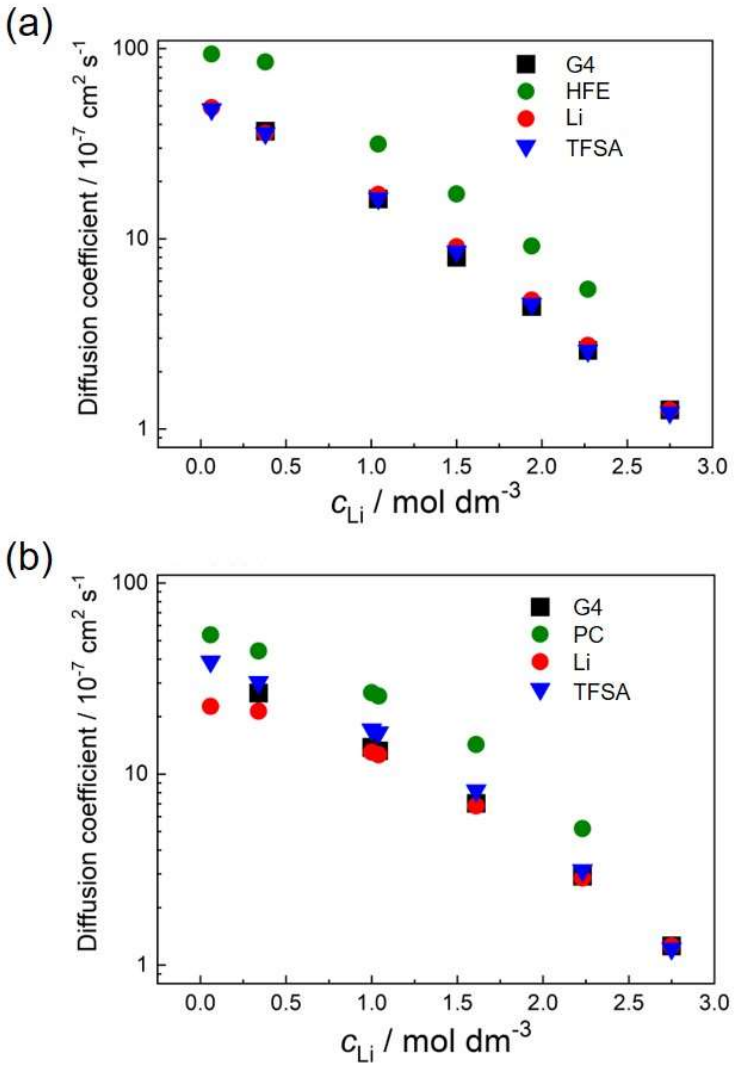

Figure 1 Concentration-dependent self-diffusion coefficients of G4, Li, TFSA, and the diluting solvents for (a) [Li(G4)][TFSA]-HFE and (b) [Li(G4)][TFSA]-PC.

3.2 Li^+ transference number

Among the several methods proposed for estimating the Li^+ transference number of Li^+-conducting electrolytes,[44] the potentiostatic polarization and diffusivity methods have been commonly employed as readily accessible experimental approaches. In the potentiostatic polarization method, the Li^+ transference

number ($t_{\mathrm{Li}}^{\mathrm{EC}}$) is obtained as a fraction of the steady-state current to the initial current, with a correction of interfacial impedance contributions in the parentheses, as follows:[35]

$$t_{\mathrm{Li}}^{\mathrm{EC}} = \frac{I_{\mathrm{SS}}(V_{\mathrm{DC}} - I_{\mathrm{Ohm}}R_{\mathrm{i},0})}{I_{\mathrm{Ohm}}(V_{\mathrm{DC}} - I_{\mathrm{SS}}R_{\mathrm{i,SS}})} \quad (\mathrm{Eq.}\,1)$$

where I_{Ohm} and I_{SS} are the initial and steady-state currents, respectively; V_{DC} is a constant applied voltage; $R_{\mathrm{i},0}$ and $R_{\mathrm{i,SS}}$ are the initial and steady-state interfacial resistances determined by electrochemical impedance spectroscopy, respectively; and I_{Ohm} is calculated from the equation $I_{\mathrm{Ohm}} = V_{\mathrm{DC}}/(R_{\mathrm{bulk}} + R_{\mathrm{i},0})$.[36, 45] Notably, $t_{\mathrm{Li}}^{\mathrm{EC}}$ may not be simply reflected by the migration of ions under an electric field: The contribution of Li-ion diffusion can be involved in the I_{SS} in the presence of a salt concentration gradient in the polarized Li/Li symmetric cell. Therefore, $t_{\mathrm{Li}}^{\mathrm{EC}}$ is not necessarily the true transference number, but is often regarded as the current fraction in non-ideal electrolyte solutions.[45] Nevertheless, $t_{\mathrm{Li}}^{\mathrm{EC}}$ is considered to be a useful parameter for screening the Li^+ transport properties of electrolyte materials in an electrochemical cell that has a similar configuration to that of Li-ion batteries (under anion-blocking conditions). In the diffusivity method based on the PFG-NMR measurement, the transference number ($t_{\mathrm{Li}}^{\mathrm{NMR}}$) is estimated as $t_{\mathrm{Li}}^{\mathrm{NMR}} = D_{\mathrm{Li}}/(D_{\mathrm{Li}} + D_{\mathrm{anion}})$. Because an ideal electrolyte solution-like behavior with complete dissociation and independent ion motions is assumed in this method, $t_{\mathrm{Li}}^{\mathrm{NMR}}$ would also not necessarily be deemed a veritable value for HCEs with significant ion-ion interactions and correlations.

In our previous work, a noticeable difference in $t_{\mathrm{Li}}^{\mathrm{EC}}$ (0.028) and $t_{\mathrm{Li}}^{\mathrm{NMR}}$(0.52) was observed for [Li(G4)][TFSA].[31] The analysis of the dynamic ion correlations using MD simulations and experimental transport properties suggested that the very low $t_{\mathrm{Li}}^{\mathrm{EC}}$ under anion-blocking conditions is due to the strongly anti-correlated ion dynamics, on account of the constraint of momentum conservation for the long-lived $[Li(G4)]^+$ complex cation and $TFSA^-$ anion in the IL-like [Li(G4)][TFSA] in which non-coordinating G4 is scarcely present.[25, 30, 31] In the MD simulation study, it was also suggested that the addition of a diluting solvent to [Li(G4)][TFSA] can reduce the negative correlations of the ion motions via the compensation

of the ion motions by freely mobile solvent motions, resulting in higher $t_{\mathrm{Li}}^{\mathrm{EC}}$. Indeed, the Li^+ transference number under anion-blocking conditions estimated in the MD simulation linearly increased from 0.06 for [Li(G4)][TFSA] to 0.5 for [Li(G4)][TFSA] diluted with excess G4 solvent.[25] The experimental transference numbers ($t_{\mathrm{Li}}^{\mathrm{EC}}$ and $t_{\mathrm{Li}}^{\mathrm{NMR}}$) of the LiTFSA-G4 solutions are shown in **Figure S3**. The data reveals that $t_{\mathrm{Li}}^{\mathrm{EC}}$ drastically increased from 0.028 for the SIL to 0.42 at the lowest c_{Li} of 0.06 mol dm^{-3}, while $t_{\mathrm{Li}}^{\mathrm{NMR}}$ slightly decreased from 0.50 to 0.45 with decreasing c_{Li}. Moreover, $t_{\mathrm{Li}}^{\mathrm{EC}}$ and $t_{\mathrm{Li}}^{\mathrm{NMR}}$ approached each other with the addition of extra G4 and became nearly identical at the lowest c_{Li}, as expected for ideal electrolyte solutions where self-correlations of ion motions dominate the transference number. The trend of the concentration-dependent changes in $t_{\mathrm{Li}}^{\mathrm{EC}}$ and $t_{\mathrm{Li}}^{\mathrm{NMR}}$ for the LiTFSA-G4 solutions is consistent with the results of the MD simulation study by Bedrov et al.[25]

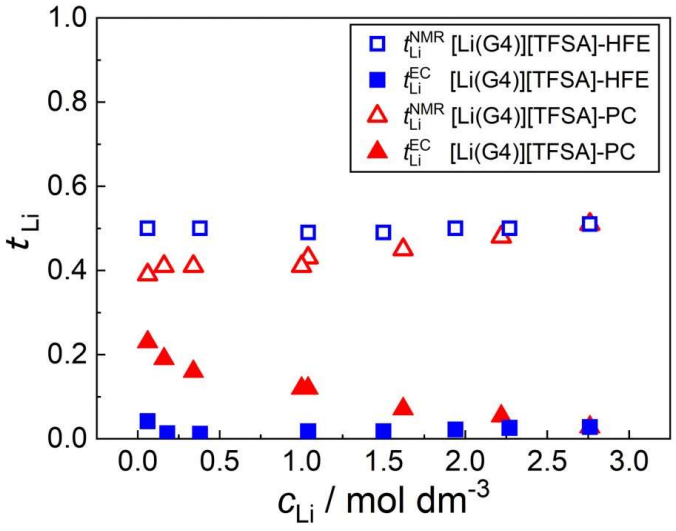

Figure 2 Concentration dependence of the Li^+ transference numbers, $t_{\mathrm{Li}}^{\mathrm{EC}}$ and $t_{\mathrm{Li}}^{\mathrm{NMR}}$, for [Li(G4)][TFSA]-HFE and [Li(G4)][TFSA]-PC .

We proceeded to examine how the addition of a low-polarity or polar diluting solvent affects the transference numbers ($t_{\mathrm{Li}}^{\mathrm{EC}}$ and $t_{\mathrm{Li}}^{\mathrm{NMR}}$) of [Li(G4)][TFSA]. **Figure 2** shows the concentration-dependent Li transference numbers of [Li(G4)][TFSA] diluted with non-coordinating HFE or coordinating PC.

Notably, the addition of HFE does not induce any significant changes in both $t_{\mathrm{Li}}^{\mathrm{EC}}$ and $t_{\mathrm{Li}}^{\mathrm{NMR}}$ within the c_{Li} range of 0.06–2.65 mol dm^{-3}—$t_{\mathrm{Li}}^{\mathrm{EC}}$ remained very low (*e.g.,* 0.018 at 1.0 mol dm^{-3}) in [Li(G4)][TFSA]-HFE. In contrast, $t_{\mathrm{Li}}^{\mathrm{EC}}$ increased to 0.12 at 1.0 mol dm^{-3} and 0.23 at 0.06 mol dm^{-3}, whereas $t_{\mathrm{Li}}^{\mathrm{NMR}}$ gradually decreased with increasing PC content in [Li(G4)][TFSA]-PC. At the lower c_{Li} values, $t_{\mathrm{Li}}^{\mathrm{EC}}$ approached $t_{\mathrm{Li}}^{\mathrm{NMR}}$, as was observed in the LiTFSA-G4 solutions (**Figure S3**) and the MD simulation study.

Evidently, the change in the transference numbers depends on the coordination properties of the diluting solvents. Unlike the prospects predicted by the previous MD simulation study[25], the above results suggest that the solvent motions of the non-coordinating HFE do not contribute to the reduction of the correlated ion motions, even though HFE is miscible with [Li(G4)][TFSA] at the macroscopic level at least. Given the increase in $t_{\mathrm{Li}}^{\mathrm{EC}}$ in the presence of coordinating diluents such as G4 and PC, whether or not the diluting solvent serves as the Li-ion solvation site would dominate the change in the transference numbers. In other words, the local Li-ion solvation structure (*i.e.*, the presence of $[\mathrm{Li(G4)}]^+$ complex cations and scarcity of free G4 for the present case) likely dictates the Li-ion transport mechanism in the LHCEs, and the $t_{\mathrm{Li}}^{\mathrm{EC}}$ and $t_{\mathrm{Li}}^{\mathrm{NMR}}$ of the LHCEs can be reflected by those of the parent HCEs. Notably, the significant effects of the coordination properties of the diluting solvents on the transference numbers have not been considered in previous studies and are demonstrated for the first time in the present work.

3.3 Dynamic ion correlations

The understanding of the ionic transport mechanism has been of significant importance for ionic conducting materials, and the cross-correlated ion motions have been investigated for aqueous electrolyte solutions[46], ionic liquids[47, 48], and solid polymer electrolytes[49-51] with both experimental and computational approaches. However, there are limited studies on the dynamic ion correlations for organic liquid electrolytes, despite their pivotal role in Li secondary batteries. Recently, Roling and Bedrov et al. examined the dynamic ion correlations of LiTFSA in glyme-based organic electrolytes including SILs, based on the concentrated electrolyte theory using the Onsager transport coefficients (σ_{++}, σ_{--}, and

σ_{+-}).[25, 30, 34] The total conductivity (σ_{ion}) can be represented by the Onsager transport coefficients as follows:

$$\sigma_{\mathrm{ion}} = \sigma_{++} + \sigma_{--} - 2\sigma_{+-} \quad \text{(Eq. 2)}.$$

Here, σ_{++} and σ_{--} are divided into self-terms and distinct terms, so that σ_{ion} is rewritten as

$$\sigma_{\mathrm{ion}} = \sigma_{+}^{\mathrm{self}} + \sigma_{++}^{\mathrm{distinct}} + \sigma_{-}^{\mathrm{self}} + \sigma_{--}^{\mathrm{distinct}} - 2\sigma_{+-} \quad \text{(Eq. 3)}.$$

The Onsager transport coefficients (σ_{++}, σ_{--}, and σ_{+-}) can be determined from the experimentally obtained transport data, including σ_{ion}, $t_{\mathrm{Li}}^{\mathrm{EC}}$, D_{salt}, the self-diffusion coefficients of Li and TFSA (D_{Li} and D_{anion}), and $\mathrm{d}\varphi/\mathrm{dln}(c)$, for a given electrolyte. These numeric data for [Li(G4)][TFSA]-HFE and [Li(G4)][TFSA]-PC solutions are listed in **Table S1**. The procedure for calculating the Onsager transport coefficients under anion-blocking conditions was described in previous literature.[25, 31] The self-terms ($\sigma_{+}^{\mathrm{self}}$ and $\sigma_{-}^{\mathrm{self}}$) are approximated using the Nernst–Einstein equation: $\sigma_{+}^{\mathrm{self}} = c_{\mathrm{Li}} D_{\mathrm{Li}} F^2/RT$ and $\sigma_{-}^{\mathrm{self}} = c_{\mathrm{Li}} D_{\mathrm{anion}} F^2/RT$, while the distinct terms can be estimated by subtracting $\sigma_{+}^{\mathrm{self}}$ and $\sigma_{-}^{\mathrm{self}}$ from σ_{++} and σ_{--}, respectively. The positive and negative sign of the distinct terms indicate correlated and anti-correlated ion motions, respectively.

Figure 3a shows the concentration dependence of the normalized transport coefficients ($\sigma/\sigma_{\mathrm{ion}}$), *i.e.*, the self and distinct terms in Eq. 3, for [Li(G4)][TFSA]-HFE. In the non-diluted [Li(G4)][TFSA], all the distinct terms are negative, indicating that the cation-cation, anion-anion, and cation-anion motions are anti-correlated because of the constraint of the momentum conservations of the $[\mathrm{Li(G4)}]^+$ complex cations and TFSA^- counter anions, as described in the former section 3.2. In [Li(G4)][TFSA]-HFE, the self-terms $\sigma_{+}^{\mathrm{self}}/\sigma_{\mathrm{ion}}$ and $\sigma_{-}^{\mathrm{self}}/\sigma_{\mathrm{ion}}$ increased with the addition of HFE. These normalized coefficients became greater than unity in the lower c_{Li} range, indicating that D_{Li} and D_{anion} do not fully contribute to the σ_{ion} values. All the distinct terms remained negative even with the addition of HFE. Moreover, $\sigma_{+-}/\sigma_{\mathrm{ion}}$ approaches to zero at the lower c_{Li} values, suggesting that anti-correlated cation-anion motions are

mitigated, to some extent, by the dilution and increased cation-anion interactions in the HFE-based low-dielectric media as shown in Raman spectra **(Figure S2**). Notably, the value of $\sigma_{++}^{\mathrm{distinct}}/\sigma_{\mathrm{ion}}$, which has a significant impact on $t_{\mathrm{Li}}^{\mathrm{EC}}$, was comparable to that of the neat [Li(G4)][TFSA], leading to the low $t_{\mathrm{Li}}^{\mathrm{EC}}$ values in [Li(G4)][TFSA]-HFE presented in **Figure 2**. In addition, $\sigma_{--}^{\mathrm{distinct}}/\sigma_{\mathrm{ion}}$ decreased with the addition of HFE. The largely negative value of $\sigma_{--}^{\mathrm{distinct}}/\sigma_{\mathrm{ion}}$ at the lower c_{Li} values is attributable to the largely positive value of $\sigma_{-}^{\mathrm{self}}/\sigma_{\mathrm{ion}}$ and near-zero value of $\sigma_{+-}/\sigma_{\mathrm{ion}}$ under the anion-blocking conditions. Consequently, the solvent motions of HFE in [Li(G4)][TFSA]-HFE cannot alleviate the anti-correlated motions of the $[\mathrm{Li(G4)}]^+$ complex cations and TFSA^- anions. Thus, the non-coordinating HFE diluents are hardly involved in the ion transport mechanism in [Li(G4)][TFSA], but merely serve as a thinner to decrease the viscosity.

The contributions of each transport coefficient in [Li(G4)][TFSA]-PC are shown in **Figure 3b**. The contribution of $\sigma_{-}^{\mathrm{self}}/\sigma_{\mathrm{ion}}$ does not change significantly in [Li(G4)][TFSA]-PC. However, $\sigma_{+}^{\mathrm{self}}/\sigma_{\mathrm{ion}}$ decreased slightly at c_{Li} values <0.5 mol dm^{-3}, owing to the change in the local Li-ion solvation structure, as discussed with $D_{\mathrm{Li}} < D_{\mathrm{G}}$ in **Figure 1b**. The marked difference from [Li(G4)][TFSA]-HFE is that $\sigma_{++}^{\mathrm{distinct}}/\sigma_{\mathrm{ion}}$ increased with the addition of the coordinating PC. This is predominantly responsible for the enhancement of $t_{\mathrm{Li}}^{\mathrm{EC}}$ in [Li(G4)][TFSA]-PC (**Figure 2**). In the diffusivity measurements, the $[\mathrm{Li(G4)}]^+$ complex cations were retained ($D_{\mathrm{Li}} \sim D_{\mathrm{G}}$) at c_{Li} values >1.0 mol dm^{-3} (**Figure 1b**). These results suggest that the solvent motions of PC can effectively suppress the anti-correlated motions of the $[\mathrm{Li(G4)}]^+$ complex cations in this region, even if the diluent is not sufficient to liberate the Li ions from the robust complex cations. At c_{Li} values <0.5 mol dm^{-3}, the $[\mathrm{Li(G4)}]^+$ complex cations were no longer considered to be stable ($D_{\mathrm{Li}} < D_{\mathrm{G}}$ in **Figure 1b**) in [Li(G4)][(TFSA)]-PC. Although we observed a slightly positive value of $\sigma_{++}^{\mathrm{distinct}}/\sigma_{\mathrm{ion}}$ in the diluted electrolyte, more frequent ligand exchange caused by competitive interactions of G4 and PC with the Li ions can facilitate more labile Li-ion transport, which was expected to lead to nearly non-correlated motions at the lower c_{Li} values. Similar to [Li(G4)][TFSA]-HFE, $\sigma_{+-}/\sigma_{\mathrm{ion}}$ approaches to zero with the addition of the diluent. The presence of the polar PC resulted in

less-pronounced anti-correlated cation-anion motions, and the further addition of PC provoked nearly non-correlated motions, as expected. This is attributed to the increased dissociation degree in the presence of PC as discussed in the former section 3.1. The negative $\sigma_{--}^{\mathrm{distinct}}/\sigma_{\mathrm{ion}}$ in [Li(G4)][(TFSA)]-PC can be ascribed to the compensation of the positive $\sigma_{-}^{\mathrm{self}}/\sigma_{\mathrm{ion}}$ under the anion-blocking conditions. Consequently, the polar PC diluent, which can solvate the Li ions, can effectively reduce the anti-correlated cation-cation and cation-anion motions, thereby improving the $t_{\mathrm{Li}}^{\mathrm{EC}}$ in [Li(G4)][TFSA]-PC. With the coordinating PC, the present study experimentally demonstrated that the anti-correlated ion dynamics can be reduced with the addition of a diluent to the SIL, as proposed by the previous MD simulations.[25]

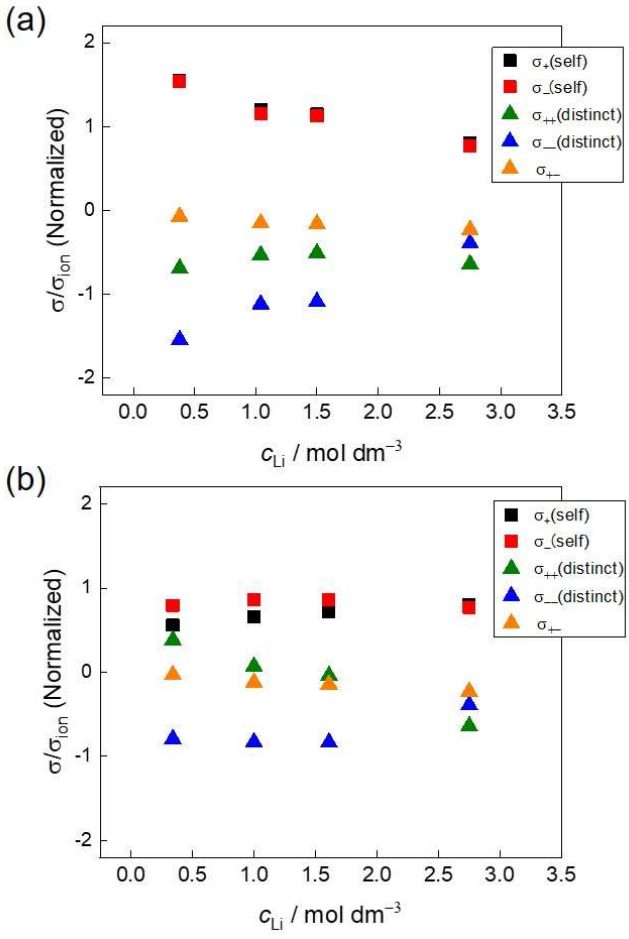

Figure 3 Concentration dependence of the normalized transport coefficients ($\sigma/\sigma_{\mathrm{ion}}$) for (a) [Li(G4)][TFSA]-HFE and (b) [Li(G4)][TFSA]-PC.

4. CONCLUSION

The Li-ion solvation structure in [Li(G4)][TFSA] diluted with HFE or PC was investigated using self-diffusion coefficient data and Raman spectra. The identical values of D_G and D_{Li} in [Li(G4)][TFSA]-HFE were indicative of the presence of $[Li(G4)]^+$ complex cations, even at a c_{Li} of 0.06 mol dm^{-3} with 100-fold dilution with HFE. In addition, no significant peak variation of Raman spectra was observed for the breathing mode of $[Li(G4)]^+$ complex cations in [Li(G4)][TFSA]-HFE solutions. Therefore, the addition of HFE does not induce a significant change in the local Li-ion solvation structure. In [Li(G4)][TFSA]-PC, the $[Li(G4)]^+$ complex cations remained stable, as suggested by the near-equivalent values of D_G and D_{Li} at c_{Li} values higher than 1.0 mol dm^{-3}. However, the ligand replacement of G4 by PC became conspicuous in [Li(G4)][TFSA]-PC at the lower c_{Li} values, which was verified by Raman spectra showing the band intensity decline of the $[Li(G4)]^+$ complex cations with the addition of PC. Both t_{Li}^{EC} and t_{Li}^{NMR} did not change in [Li(G4)][TFSA]-HFE within the studied c_{Li} range, whereas in [Li(G4)][TFSA]-PC, the two values increased and decreased, respectively, with the addition of PC. Analysis of the dynamic ion correlations suggested that the addition of non-coordinating diluents such as HFE does not alter the ion transport mechanism nor reduce the anti-correlated ion motions, unlike the predictions of the previous MD simulations. In contrast, coordinating diluents such as G4 and PC allow the suppression of the anti-correlated cation-cation and cation-anion motions for [Li(G4)][TFSA], leading to the improvement of t_{Li}^{EC}. However, the addition of a coordinating diluent also causes the collapse of the unique Li-ion solvation structure, which in turn can lead to unfavorable electrochemical properties. These observations can be expanded to other LHCEs using a non-coordinating diluent and provide further insight into the electrolyte design of LHCEs for next-generation batteries. Because the t_{Li}^{EC} of HCEs can be inherited by the LHCEs, mixtures of HCEs with intrinsically high t_{Li}^{EC} values and non-coordinating diluents would be more efficient for finding an appropriate balance between ion transport (σ_{ion} and t_{Li}^{EC}) and the electrochemical properties.

Conflicts of interest:

There are no conflicts of interest to declare.

ACKNOWLEDGMENT: This study was supported in part by the Japan Society for the Promotion of Science (JSPS) KAKENHI (Grant No. 20H02837 to K. U., and 18H03926 to K. D.), JST ALCA-SPRING (Grant Number JPMJAL1301), Japan. This study is also based on results obtained from a project, JPNP20004, subsidized by the New Energy and Industrial Technology Development Organization (NEDO).

Supplementary Information: Plots of the Li/Li$^+$ electrode potential for the diluted [Li(G4)][TFSA]; Raman spectra of [Li(G4)][TFSA]-HFE and [Li(G4)][TFSA]-PC solutions; concentration dependence of the Li transference numbers, $t_{\mathrm{Li}}^{\mathrm{EC}}$ and $t_{\mathrm{Li}}^{\mathrm{NMR}}$, for the LiTFSA-G4 solutions; salt concentration and six experimentally obtained parameters for calculating the Onsager transport coefficients; and normalized five transport coefficients of all the electrolytes at 30 °C.

References

1. K. Xu, *Chem. Rev.*, 2014, **114**, 11503-11618.
2. Y. Yamada and A. Yamada, *J. Electrochem. Soc.*, 2015, **162**, A2406-A2423.
3. Y. Yamada, J. Wang, S. Ko, E. Watanabe and A. Yamada, *Nat. Energy*, 2019, **4**, 269-280.
4. K. Yoshida, M. Nakamura, Y. Kazue, N. Tachikawa, S. Tsuzuki, S. Seki, K. Dokko and M. Watanabe, *J. Am. Chem. Soc.*, 2011, **133**, 13121-13129.
5. J. Wang, Y. Yamada, K. Sodeyama, C. H. Chiang, Y. Tateyama and A. Yamada, *Nat. Commun.*, 2016, **7**, 12032.
6. Y. Yamada, M. Yaegashi, T. Abe and A. Yamada, *Chem. Commun.*, 2013, **49**, 11194-11196.
7. X. Gao, F. Wu, A. Mariani and S. Passerini, *ChemSusChem*, 2019, **12**, 4185-4193.
8. M. Forsyth, H. Yoon, F. Chen, H. Zhu, D. R. MacFarlane, M. Armand and P. C. Howlett, *J. Phys. Chem. C*, 2016, **120**, 4276-4286.
9. H. Yoon, P. C. Howlett, A. S. Best, M. Forsyth and D. R. MacFarlane, *J. Electrochem. Soc.*, 2013, **160**, A1629-A1637.
10. D. W. McOwen, D. M. Seo, O. Borodin, J. Vatamanu, P. D. Boyle and W. A. Henderson, *Energy Environ. Sci.*, 2014, **7**, 416-426.
11. Y. Yamada, C. H. Chiang, K. Sodeyama, J. Wang, Y. Tateyama and A. Yamada, *ChemElectroChem*, 2015, **2**, 1687-1694.
12. K. Dokko, N. Tachikawa, K. Yamauchi, M. Tsuchiya, A. Yamazaki, E. Takashima, J.-W. Park, K. Ueno, S. Seki, N. Serizawa and M. Watanabe, *J. Electrochem. Soc.*, 2013, **160**, A1304-A1310.
13. L. Suo, Y.-S. Hu, H. Li, M. Armand and L. Chen, *Nat. Commun.*, 2013, **4**, 1481.
14. E. S. Shin, K. Kim, S. H. Oh and W. I. Cho, *Chem. Commun.*, 2013, **49**, 2004-2006.
15. T. Mandai, K. Yoshida, K. Ueno, K. Dokko and M. Watanabe, *Phys. Chem. Chem. Phys.*, 2014, **16**, 8761-8772.
16. K. Ueno, K. Yoshida, M. Tsuchiya, N. Tachikawa, K. Dokko and M. Watanabe, *J. Phys. Chem. B*, 2012, **116**, 11323-11331.
17. S. Tsuzuki, W. Shinoda, M. Matsugami, Y. Umebayashi, K. Ueno, T. Mandai, S. Seki, K. Dokko and M. Watanabe, *Phys. Chem. Chem. Phys.*, 2015, **17**, 126-129.
18. K. Shimizu, A. A. Freitas, R. Atkin, G. G. Warr, P. A. FitzGerald, H. Doi, S. Saito, K. Ueno, Y. Umebayashi, M. Watanabe and J. N. Canongia Lopes, *Phys. Chem. Chem. Phys.*, 2015, **17**, 22321-22335.
19. S. Saito, H. Watanabe, Y. Hayashi, M. Matsugami, S. Tsuzuki, S. Seki, J. N. Canongia Lopes, R. Atkin, K. Ueno, K. Dokko, M. Watanabe, Y. Kameda and Y. Umebayashi, *J. Phys. Chem. Lett.*, 2016, **7**, 2832-2837.
20. W. Shinoda, Y. Hatanaka, M. Hirakawa, S. Okazaki, S. Tsuzuki, K. Ueno and M. Watanabe, *J. Chem. Phys.*, 2018, **148**, 193809.
21. K. Ueno, J. Murai, K. Ikeda, S. Tsuzuki, M. Tsuchiya, R. Tatara, T. Mandai, Y. Umebayashi, K. Dokko and M. Watanabe, *J. Phys. Chem. C*, 2016, **120**, 15792-15802.
22. M. Cuisinier, P. E. Cabelguen, B. D. Adams, A. Garsuch, M. Balasubramanian and L. F. Nazar, *Energy Environ. Sci.*, 2014, **7**, 2697-2705.
23. X. Cao, H. Jia, W. Xu and J.-G. Zhang, *J. Electrochem. Soc.*, 2021, **168**, 010522.
24. X. Ren, S. Chen, H. Lee, D. Mei, M. H. Engelhard, S. D. Burton, W. Zhao, J. Zheng, Q. Li, M. S. Ding, M. Schroeder, J. Alvarado, K. Xu, Y. S. Meng, J. Liu, J.-G. Zhang and W. Xu, *Chem*, 2018, **4**, 1877-1892.
25. D. Dong, F. Sälzer, B. Roling and D. Bedrov, *Phys. Chem. Chem. Phys.*, 2018, **20**, 29174-29183.
26. F. Schmidt and M. Schönhoff, *J. Phys. Chem. B*, 2020, **124**, 1245-1252.
27. H. K. Kashyap, H. V. Annapureddy, F. O. Raineri and C. J. Margulis, *J. Phys. Chem. B*, 2011, **115**, 13212-13221.
28. K. R. Harris and M. Kanakubo, *J. Chem. Eng. Data*, 2016, **61**, 2399-2411.

29. A. D. McNaught and A. Wilkinson, *Compendium of chemical terminology*, Blackwell Science Oxford, 1997.
30. F. Wohde, M. Balabajew and B. Roling, *J. Electrochem. Soc.*, 2016, **163**, A714-A721.
31. K. Shigenobu, K. Dokko, M. Watanabe and K. Ueno, *Phys. Chem. Chem. Phys.*, 2020, **22**, 15214-15221.
32. M. Doyle, T. F. Fuller and J. Newman, *Electrochim. Acta*, 1994, **39**, 2073-2081.
33. K. M. Diederichsen, E. J. McShane and B. D. McCloskey, *ACS Energy Lett.*, 2017, **2**, 2563-2575.
34. N. M. Vargas-Barbosa and B. Roling, *ChemElectroChem*, 2020, **7**, 367-385.
35. P. G. Bruce, J. Evans and C. A. Vincent, *Solid State Ionics*, 1988, **28-30**, 918-922.
36. M. Watanabe, S. Nagano, K. Sanui and N. Ogata, *Solid State Ionics*, 1988, **28-30**, 911-917.
37. D. Brouillette, G. Perron and J. E. Desnoyers, *J. Solution Chem.*, 1998, **27**, 151-182.
38. S. Saito, H. Watanabe, K. Ueno, T. Mandai, S. Seki, S. Tsuzuki, Y. Kameda, K. Dokko, M. Watanabe and Y. Umebayashi, *J. Phys. Chem. B*, 2016, **120**, 3378-3387.
39. H. Moon, T. Mandai, R. Tatara, K. Ueno, A. Yamazaki, K. Yoshida, S. Seki, K. Dokko and M. Watanabe, *J. Phys. Chem. C*, 2015, **119**, 3957-3970.
40. K. Hayamizu, Y. Aihara, S. Arai and C. G. Martinez, *J. Phys. Chem. B*, 1999, **103**, 519-524.
41. K. Hayamizu, *J. Chem. Eng. Data*, 2012, **57**, 2012-2017.
42. E. Cazzanelli, F. Croce, G. B. Appetecchi, F. Benevelli and P. Mustarelli, *J. Chem. Phys.*, 1997, **107**, 5740-5747.
43. K. Ueno, J. Murai, H. Moon, K. Dokko and M. Watanabe, *J. Electrochem. Soc.*, 2016, **164**, A6088-A6094.
44. S. Zugmann, M. Fleischmann, M. Amereller, R. M. Gschwind, H. D. Wiemhöfer and H. J. Gores, *Electrochim. Acta*, 2011, **56**, 3926-3933.
45. M. D. Galluzzo, J. A. Maslyn, D. B. Shah and N. P. Balsara, *J. Chem. Phys.*, 2019, **151**, 020901.
46. L. A. Woolf and K. R. Harris, *J. Chem. Soc., Faraday Trans. 1*, 1978, **74**, 933-947.
47. J. G. McDaniel and C. Y. Son, *J. Phys. Chem. B*, 2018, **122**, 7154-7169.
48. P. Nürnberg, J. Atik, O. Borodin, M. Winter, E. Paillard and M. Schönhoff, *J. Am. Chem. Soc.*, 2022, **144**, 4657-4666.
49. D. M. Pesko, K. Timachova, R. Bhattacharya, M. C. Smith, I. Villaluenga, J. Newman and N. P. Balsara, *J. Electrochem. Soc.*, 2017, **164**, E3569-E3575.
50. D. B. Shah, H. Q. Nguyen, L. S. Grundy, K. R. Olson, S. J. Mecham, J. M. DeSimone and N. P. Balsara, *Phys. Chem. Chem. Phys.*, 2019, **21**, 7857-7866.
51. I. Villaluenga, D. M. Pesko, K. Timachova, Z. Feng, J. Newman, V. Srinivasan and N. P. Balsara, *J. Electrochem. Soc.*, 2018, **165**, A2766-A2773.